Stress Concentration Analysis in Fibre-reinforced Ceramic Components

W. Hufenbach

Department of Applied and Material Mechanics at the Institute of Technical Mechanics,
Technical University of Clausthal, W-3392 Clausthal-Zellerfeld, Germany

Abstract

When using technical ceramics in highly strained structured components, importance is attached to the tensional stress concentrations, as they are found at circular holes or notches of other shapes. These stress concentrations lead to critical strains and frequently initiate catastrophic failure of the component. By selective fibre reinforcement of the matrix a redistribution of the stress peaks relevant to failure can be achieved. In the course of this the fibre orientation, besides the notch geometry, plays a decisive role.

The basis for the dimensioning of fibre-reinforced ceramic components are the so-called 'characteristic value functions' which can be illustrated quite practically in polar diagrams.

In an example of a fibre-reinforced plain ceramic structure, the stress-induced tensional fields will be calculated by analytical and numerical means for technically relevant hole geometries. This will be accompanied by the determination of the stress concentration factors and the graphic display of these results.

Beim Einsatz von Ingenieurkeramiken für hochbeanspruchte Bauteilstrukturen kommt vor allem den Zugspannungskonzentrationen—wie sie zum Beispiel an Kreislöchern und anderen Kerbformen auftreten— besondere Bedeutung zu. Sie führen zu kritischen Beanspruchungen und initiieren häufig das Bauteilversagen. Durch gezielte Faserverstärkung der keramischen Matrix läßt sich eine Umlagerung versagensrelevanter Spannungsspitzen erreichen, wobei neben der Kerbgeometrie auch der Faserorientierung eine entscheidende Rolle zufällt.

Grundlage für die Dimensionierung faserverstärkter keramischer Bauteile bilden sogenannte 'Kennwertfunktionen', deren Darstellung in Polardiagrammen sich als recht praktikabel erweist.

Am Beispiel einer faserverstärkten ebenen Keramikstruktur werden für technisch relevante Kerbgeometrien die induzierten Spannungsfelder mittels analytischer und numerischer Verfahren berechnet, die Kerbspannungsfaktoren ermittelt und die Ergebnisse graphisch dargestellt.

Dans l'utilisation des corps céramiques comme éléments de construction exposés aux grandes forces, l'importance est avant tout attachée aux zones de concentration de tension comme elles se présentent aux troux circulaires et aux coches d'autres formes. Elles menent aux efforts critiques qui conduisent souvent à la déstruction de l'élément de construction. Par le renforcement de la matrice céramique à fibres, on peut ainsi atteindre une rédistribution de sommets de tension pertinents à la défaillance; aussi bien que l'orientation des fibres, la géometrie de la coche joue un rôle décisif dans cette rédistribution.

La base du dimensionnement des élements en céramiques renforcées à fibres avec des coches conceptionelles forment ce qu'on appelle 'fonctions à valeurs caractéristiques' qui peuvent bien être illustrées sur des diagrammes polaires.

Dans l'exemple d'une structure plane en céramique renforcée à fibres, les champs de tension induite pour des coches pertinantes techniquement sont déterminés au moyen des méthodes analytiques et numériques; les facteurs de concentration de tension sont aussi calculés et exposés graphiquement.

1 Introduction

Ceramic parts based on Si_3N_4, SiC as well as Al_2O_3 and ZrO_2 are being employed to an increasing extent in highly strained structural components subjected to high loads at high temperatures, as well as wear or

corrosion.[1] A decisive factor for the successful application of such components is a design that takes the special mechanical properties of ceramics, such as brittleness, into account. In this class of materials, tension peaks cannot be relieved by plastic deformation. Especially high tensile stresses often result in critical strains on the material and ultimately initiate catastrophic failure of the component.

Such stress concentrations in ceramic parts with circular, elliptical or square holes, as required by constructive measures, can result in failure of the parts even under small externally applied loads. The knowledge of the stress–strain field around holes is therefore of utmost importance for the design engineer concerned with ceramics, as well as for the technologist.

The reduction of the sensitivity to brittle fracture is an essential goal in the further development of high-tech ceramics.[2] One of the most promising methods of increasing toughness is based on the incorporation of endless fibres. Such a composite material permits redistribution of local stress peaks around the hole by selective fibre reinforcement, which is influenced chiefly by the fibre–matrix combination and interaction, the shape of the hole, the orientation of the fibre towards the applied load direction, and the kind of loading.

The basis for the correct dimensioning of fibre-reinforced ceramic components with anisotropic property profiles is the so-called 'characteristic value functions'. Their orientation-dependent projection in polar coordinates has proved to be quite practical. For the design engineer, these projections allow immediate access to all mechanical properties of the fibre-reinforced material to be used in a construc-

Table 1. Average material constants for fibre and matrix materials

	ρ (g/cm^3)	$E_\parallel$ (GPa)	$E_\perp$ (GPa)	$\nu_{\parallel\perp}$	G_* (GPa)
Fibre					
C fibre HT	1·78	240	15	0·28	50
C fibre HM	1·96	500	5·7	0·36	18
SiC fibre (Nicalon)	2·55	200			77
SiC fibre (Tyranno)	2·40	200			
Al₂O₃ fibre (Nextel 480)	2·3		224		
Al₂O₃ fibre (Safimax)	3·30		300		
Aramid fibre HM	1·45	140	5·4	0·38	12
Glass fibre E	2·45		73	0·25	29
Glass fibre R	2·48		84	0·25	34
Matrix					
Al₂O₃	3·10		330	0·23	
SiC	3·21		360	0·18	
Si₃N₄					
HPSN	3·25		320	0·28	
RBSN	2·5		180	0·23	
SSN	3·2		290	0·20	
ZrO₂	5·8		200	0·26	
LAS glass ceramic	2·5		88	0·16	38
Borosilicate glass	2·5		68	0·2	28
EP resin	1·22		3·6	0·35	1·3
Polyamid 6	1·12		1·4	0·38	0·5
Aluminium	2·70		70	0·30	27
Steel	7·85		210	0·30	81

Abbreviation	*Definition*
ρ	density
$E_\parallel$, $E_\perp$	Young's moduli parallel ($\parallel$) and perpendicular ($\perp$) to fibre direction, respectively
$\nu_{\parallel\perp}$	Poisson's ratio for transverse strain perpendicular to fibre direction when stressed in fibre direction
G_*	shear modulus
HT	High Tenacity
HM	High Modulus
Glass fibre E or R	special types of glass fibres
HPSN	hot-pressed silicon nitride
RBSN	reaction-bonded silicon nitride
SSN	sintered silicon nitride
LAS	lithium-alumino-silicate
EP resin	epoxy resin

tion; this feature provides a useful tool for designing ceramic components.

In an example of a fibre-reinforced plain ceramic structure, the stress-induced tensional fields will be calculated by analytical and numerical means for technically relevant hole geometries. This will be accompanied by the determination of the stress concentration factors and the graphic display of these results.

2 The Principles of Reinforcement and Fibre Selection

To reinforce ceramic materials one can incorporate short fibres, platelets, whiskers, or partially stabilized zirconia particles. A considerable increase in toughness can also be achieved by the incorporation of continuous fibres.[3] It is important to point out that, contrary to fibre-reinforced polymers, the fracture strain in fibre-reinforced ceramic matrices is of the same order as that of the fibres themselves. Therefore, microstructural tension peaks cannot be relieved because of the deformation restraints of the matrix, which results in a limitation of the achievable increase in strength. Hence, the primary objective of the reinforcement is the improvement of the toughness of the brittle monolithic ceramic body. Generally, the reinforcement results in a dependence of the toughness and strength on the orientation.[4]

Recently, reinforcing fibres for glass, glass ceramics and ceramics have been made predominantly of SiC and C. Furthermore, glass fibres especially for the reinforcement of monolithic glasses and alumina fibres have come into use.[5] The application of carbon fibres is limited to reducing atmospheres, because of their limited resistance to oxidation at high temperatures. In this environment, SiC fibres, which are less susceptible to oxidation, offer decided advantages.[6]
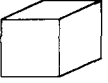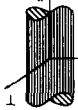
component	material	number of independent basic elasticity constants		
matrix	- isotropic - homogeneous ceramics, glass ceramics, glass, metal, polymer	2		E, v, $G = \dfrac{E}{2(1+v)}$
fibre	- isotropic - homogeneous glass fibre alumina fibre	2		E, v, $G = \dfrac{E}{2(1+v)}$
	- orthotropic transversal isotropic - homogeneous C fibre SiC fibre aramid fibre	5		$E_{\parallel}$, $E_{\perp}$, $v_{\parallel\perp}$, $v_{\perp\perp}$, $G_{\parallel}$, $G_{\perp\perp} = \dfrac{E_{\perp}}{2(1+v_{\perp\perp})}$

Fig. 1. Mechanical properties of composite components.

As matrix material, SiC also exhibits excellent properties, especially as a result of high compatibility with SiC and C fibres, as well as excellent resistance to thermal shock. In Table 1 the basic specific elasticity values for essential matrix and fibre materials are given in relation to Fig. 1.

3 Basis for Calculations

The absolute command and use of the property profile of fibre-reinforced ceramics require a broad knowledge of the structural mechanical interconnections in dealing with anisotropic materials on the part of the design engineer.

In dimensioning of fibre-ceramic compound components, continuous space approaches of mechanics are used as basis for mathematical treatment. In the course of this phenomenological continuum approach the microstructural heterogeneous material structure will be treated macroscopically by the homogenization technique.

4 Elasticity Rules for Anisotropic Materials

The material behaviour of fibre-reinforced materials can be described by the tensor notation of Hooke's law,

$$\sigma_{ij} = C_{ijkl} \cdot \varepsilon_{kl} \quad (i,j,k,l = 1,2,3) \tag{1}$$

where C_{ijkl} represents a fourth-order material tensor with 81 constants. With the assumption of symmetry among the stress and strain tensor components, the 81 constants reduce to 36 independent values. The law of elasticity can therefore be written in a 'pseudovectorial' manner as:

$$\sigma_i = C_{ik} \cdot \varepsilon_k \quad (i,k = 1,2,\dots,6) \tag{2}$$

With the assumption of an existing elastic potential, which is regarded as a unique function of the strain tensor components, one can state:

$$C_{ik} = C_{ki} \quad (i,k = 1,2,\dots,6) \tag{3}$$

This reduces the number of elastic constants to 21.

In technically relevant fibre-reinforced ceramics, a texture exists with respect to three independent, mutually perpendicular directions. In terms of crystal chemistry, this case is called orthorhombic anisotropy or orthotropy. This results in a material tensor consisting of 12 components, of which 9 are linearly independent of each other. Finally, one can express the material law (eqn (2)) for a three-dimensional orthotropic body within the system of

the main axes for the material in the following form:

$$\begin{bmatrix} \sigma_1 \\ \sigma_2 \\ \sigma_3 \\ \tau_{23} \\ \tau_{13} \\ \tau_{12} \end{bmatrix} = \begin{bmatrix} C_{11} & C_{12} & C_{13} & 0 & 0 & 0 \\ C_{12} & C_{22} & C_{23} & 0 & 0 & 0 \\ C_{13} & C_{23} & C_{33} & 0 & 0 & 0 \\ 0 & 0 & 0 & C_{44} & 0 & 0 \\ 0 & 0 & 0 & 0 & C_{55} & 0 \\ 0 & 0 & 0 & 0 & 0 & C_{66} \end{bmatrix} \begin{bmatrix} \varepsilon_1 \\ \varepsilon_2 \\ \varepsilon_3 \\ \gamma_{23} \\ \gamma_{13} \\ \gamma_{12} \end{bmatrix} \quad (4)$$

For the planar problem considered in this work, the assumption of an approximately plane stress distribution is allowed; thus eqn (4) results in:

$$\begin{bmatrix} \sigma_1 \\ \sigma_2 \\ \tau_{12} \end{bmatrix} = \begin{bmatrix} Q_{11} & Q_{12} & 0 \\ Q_{12} & Q_{22} & 0 \\ 0 & 0 & Q_{66} \end{bmatrix} \begin{bmatrix} \varepsilon_1 \\ \varepsilon_2 \\ \gamma_{12} \end{bmatrix} \quad (5)$$

The Q_{ij} represent the so-called reduced stiffnesses, which can be expressed in accordance with:

$$Q_{ij} = C_{ij} - \frac{C_{i3} \cdot C_{j3}}{C_{33}} \quad (i,j = 1,2,6) \quad (6)$$

When solved for the strains, eqn (5) yields the following expressions:

$$\begin{aligned} \varepsilon_1 &= \sigma_1 S_{11} + \sigma_2 S_{12} \\ \varepsilon_2 &= \sigma_1 S_{12} + \sigma_2 S_{22} \\ \gamma_{12} &= \tau_{12} S_{66} \end{aligned} \quad (7)$$

The connection between the compliances S_{ij} and the engineering parameters (compare with Fig. 2) is given by

$$S_{11} = \frac{1}{E_\parallel}$$

$$S_{12} = -\frac{v_{\parallel\perp}}{E_\parallel} = -\frac{v_{\perp\parallel}}{E_\perp} = S_{21} \quad (8)$$

$$S_{22} = \frac{1}{E_\perp}$$

$$S_{66} = \frac{1}{G_*}$$

5 Transformation Relations

In order to determine the stress–strain relationship for an orthotropic plane structure within a global $\tilde{x}_1$, $\tilde{x}_2, \tilde{x}_3$ system of coordinates (Fig. 2), one has to apply a polar transformation to the stresses and strains as well as to the stiffnesses and compliances known for the x_1, x_2, x_3 main axes system. The following equations describe the transformation behaviour of a
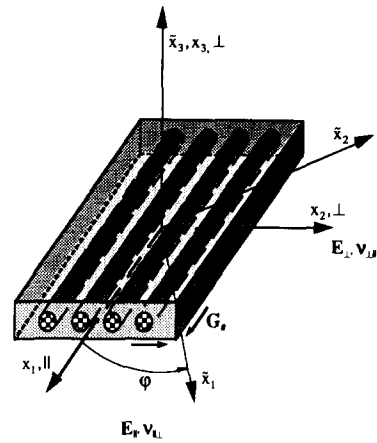

Fig. 2. Elastic constants in the main axes system of the material x_1, x_2, x_3.

coordinate system rotated by an angle φ from the fibre direction in a mathematically positive sense:

$$\begin{aligned} \tilde{C} &= T \cdot C \cdot T^T \\ \tilde{S} &= T^{-T} \cdot S \cdot T^{-1} \\ \tilde{\sigma} &= T \cdot \sigma \\ \tilde{\varepsilon} &= T \cdot \varepsilon \end{aligned} \quad (9)$$

where

$$T = \begin{bmatrix} \cos^2\varphi & \sin^2\varphi & 2\sin\varphi\cos\varphi \\ \sin^2\varphi & \cos^2\varphi & -2\sin\varphi\cos\varphi \\ -\sin\varphi\cos\varphi & \sin\varphi\cos\varphi & \cos^2\varphi - \sin^2\varphi \end{bmatrix}$$

The illustration of the transformation correlations (eqn (9)) provides the design engineer with quite practical polar diagrams, which allow an immediate reading of the interrelation between the material constants oriented parallel to the main axes (basic constants $E_\parallel$, $E_\perp$, $v_{\parallel\perp}$, G_*) and the constants rotated by any angle φ with respect to the main axes; in Fig. 3 the elastic moduli of a SiC-reinforced glass ceramic[7] and carbon-fibre-reinforced carbon (CFC) are given as examples.

6 Mathematical Treatment of the Stress Distribution Around a Notch

With the assumptions of an anistropic material law as well as a plane stress field, the following bipotential equation, often designated as 'anisotropic plane equation', is valid:

$$\tilde{S}_{11}\frac{\partial^4 F}{\partial \tilde{x}_2^4} - 2\tilde{S}_{16}\frac{\partial^4 F}{\partial \tilde{x}_1 \partial \tilde{x}_2^3} + (2\tilde{S}_{12} + \tilde{S}_{66})\frac{\partial^4 F}{\partial \tilde{x}_1^2 \partial \tilde{x}_2^2}$$

$$-2\tilde{S}_{26}\frac{\partial^4 F}{\partial \tilde{x}_1^3 \partial \tilde{x}_2} + \tilde{S}_{22}\frac{\partial^4 F}{\partial \tilde{x}_1^4} = 0 \quad (10)$$
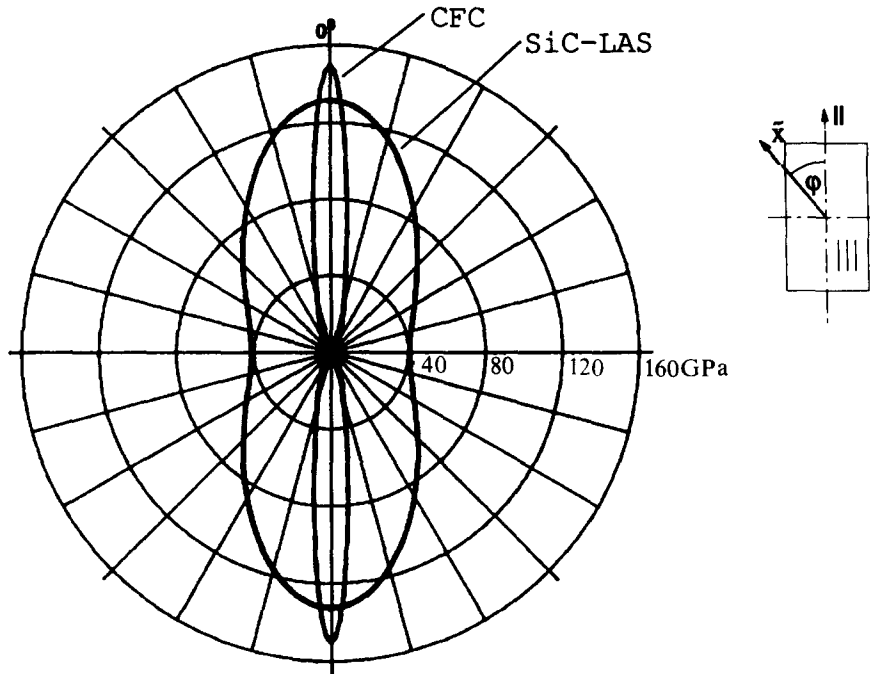
Fig. 3. Polar diagram of the elastic modulus of CFC and a SiC fibre-reinforced lithium aluminosilicate glass ceramic (LAS). Material constants CFC: $E_{\parallel} = 150\,\text{GPa}$; $E_{\perp} = 3 \cdot 1\,\text{GPa}$; $v_{\parallel\perp} = 0 \cdot 35$; $G_* = 2\,\text{GPa}$; material constants SiC-LAS: $E_{\parallel} = 132\,\text{GPa}$; $E_{\perp} = 41\,\text{GPa}$; $v_{\parallel\perp} = 0 \cdot 18$; $G_* = 30\,\text{GPa}$.

where the Airy stress function F is introduced as follows:

$$\sigma_1 = \frac{\partial^2 F}{\partial \tilde{x}_2^2}$$

$$\sigma_2 = \frac{\partial^2 F}{\partial \tilde{x}_1^2}$$

$$\tau_{12} = -\frac{\partial^2 F}{\partial \tilde{x}_1\,\partial \tilde{x}_2} \qquad (11)$$

In the case of orthotropic behaviour considered here, eqn (10) reduces to

$$S_{11}\frac{\partial^4 F}{\partial x_2^4} + (2S_{12} + S_{66})\frac{\partial^4 F}{\partial x_1^2\,\partial x_2^2} + S_{22}\frac{\partial^4 F}{\partial x_1^4} = 0 \qquad (12)$$

(x_1 parallel, x_2 perpendicular to the fibre direction). In the case of isotropy the following equation is obtained:

$$\Delta\,\Delta F \equiv \frac{\partial^4 F}{\partial x_1^4} + 2\frac{\partial^4 F}{\partial x_1^2\,\partial x_2^2} + \frac{\partial^4 F}{\partial x_2^4} = 0 \qquad (13)$$

In this case, no material constant is introduced into the bipotential equation, in contrast to the aniso-tropic plane equation. From eqn (12) in combination with the stated Airy stress function

$$F = f(x_1 + \mu x_2) \qquad (14)$$

the characteristic equation follows:

$$\mu^4 + \frac{2S_{12} + S_{66}}{S_{11}}\mu^2 + \frac{S_{22}}{S_{11}} = 0 \qquad (15)$$

For all materials used in practical applications, the solutions of eqn (15) for μ are pairs of conjugated complex values and are therefore designated as complex material constants. The analytical functions eqn (14) formed with the aid of these constants are solutions for the Airy function F which, after appropriate adjustment of the boundary conditions, permit the calculation of the stress field of a notched plate.

The tensional state of the solid plate, perturbed by the cutout, in accordance with the principle of superposition, can be interpreted as the super-position (Fig. 4) of an unperturbed strained state of the solid plate and the perturbed state of the hole, which, at a sufficient distance from the notch, has no more influence on the stresses.

For the unperturbed state, the natural boundary conditions have to be considered. In the case of the perturbed state the conditions at the rim of the notch must be fulfilled. For practical calculation, the method of conformal projection has proved to be the most advantageous. With this method, the outline of the notch is projected onto a unit circle. Analytical and experimental investigations in the field of notched fibre-reinforced plates of polymeric materials can be found in Refs 9–11.

From the evaluated stress function, F, one can calculate the stress components with the use of eqn (11). If transformation eqn (9) is applied to these components, they can be transformed to a natural
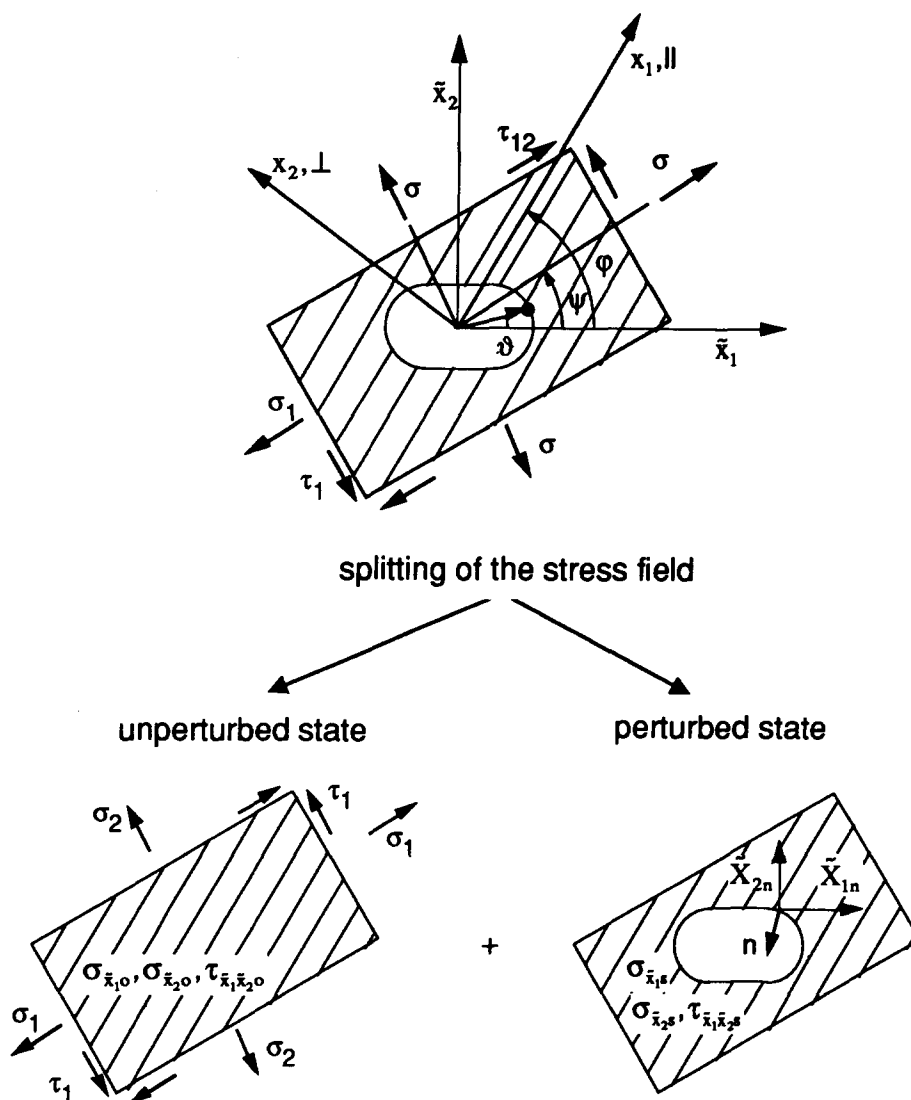
Fig. 4. Splitting of the stress problem.[8] φ, Angle to fibre-oriented system; ψ, angle to load direction; ϑ, rim parameter.

coordinate system which is tangential and normal to the outline of the hole. In analogy with this, the stress field can be determined for other materials and hole geometries. An arbitrary choice of geometries, loads and material-specific constants is possible.[12,13]

To judge the stress concentration at the notch, the stress concentration factor α, which is known for isotropic materials, is formally transferred to anisotropic materials. This value characterizes the ratio of the notch stress to the nominal stress (α normalized stress concentration factor). Because it is independent of the magnitude of the applied load, it is a valuable figure for dimensioning of components.[14]

In Figs 5 and 6, diagrams of the stress concentration factors are shown for anisotropic plates made of CFC and carbon-fibre-reinforced borosilicate glass under tension. As a basis for the model calculation, the dimension of the plate is assumed to

be infinite in comparison with the various hole geometries. In the representation related to the hole, the stress concentration factors are plotted normal to the shape of the notch, which specifies the zero level of the tangential stress. They are plotted against the notch rim parameter ϑ. Tensile stresses point outward in the diagrams, whereas compressive stresses point inward. The load direction is symbolized by the arrows **P** and by the angle ψ (as indicated in Fig. 4). The angle φ is the angle included between the orthotropic main axis of the maximum elastic modulus and the abscissa of the plotted global coordinate system. For comparison, the known stress concentration factors for the isotropic case are plotted as thin lines

The decrease of the local stress concentration maxima is depicted in Fig. 7. This characteristic is of vital importance for design decisions, since it indicates the scope of critical stress intensities.[16]
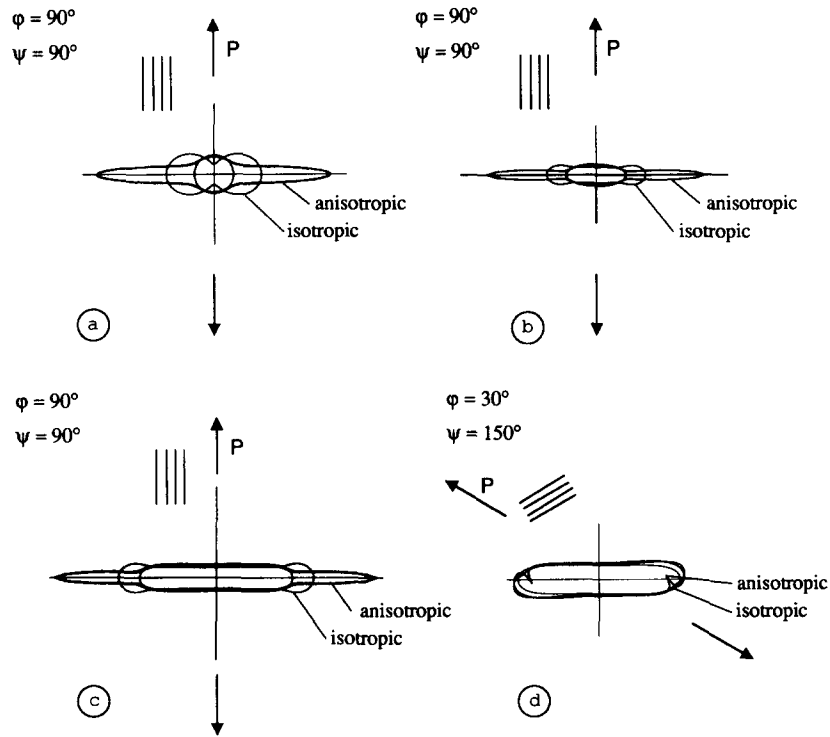
$\varphi = 90°$
$\psi = 90°$
P
anisotropic
isotropic
(a)

$\varphi = 90°$
$\psi = 90°$
P
anisotropic
isotropic
(b)

$\varphi = 90°$
$\psi = 90°$
P
anisotropic
isotropic
(c)

$\varphi = 30°$
$\psi = 150°$
P
anisotropic
isotropic
(d)

Fig. 5. Stress concentration factor α for loading in the direction of the main orthotropic axes: (a) Circular notch, $\alpha_{max} = 10\cdot39$ for $\vartheta = 0°$; (b) elliptic notch, $\alpha_{max} = 24\cdot48$ for $\vartheta = 0$; stress concentration factor α for an oblong hole: (c) On-axis loading, $\alpha_{max} = 28\cdot62$ for $\vartheta = 0°$; (d) off-axis loading, $\alpha_{max} = 2\cdot85$ for $\vartheta = 5\cdot85°$; $\alpha_{min} = -8\cdot05$ for $\vartheta = 172\cdot5°$. Material constants CFC: $E_{||} = 150\,\mathrm{GPa}$; $E_{\perp} = 3\cdot1\,\mathrm{GPa}$; $v_{||\perp} = 0\cdot35$; $G_{*} = 2\,\mathrm{GPa}$.

$\varphi = 90°$
$\psi = 90°$
P
anisotropic
isotropic
(a)

$\varphi = 90°$
$\psi = 90°$
P
anisotropic
isotropic
(b)

$\varphi = 90°$
$\psi = 90°$
P
anisotropic
isotropic
(c)

$\varphi = 30°$
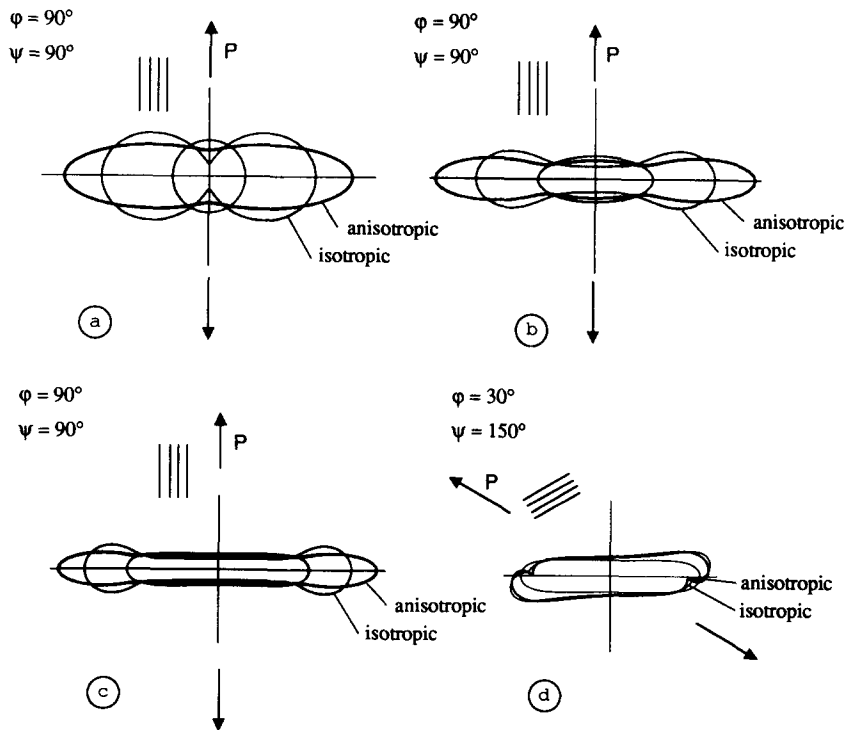$\psi = 150°$
P
anisotropic
isotropic
(d)

Fig. 6. Stress concentration factor α for loading in the direction of the main orthotropic axes: (a) Circular notch, $\alpha_{max} = 4\cdot58$ for $\vartheta = 0°$; (b) elliptic notch, $\alpha_{max} = 9\cdot94$ for $\vartheta = 0°$; stress concentration factor α for an oblong hole: (c) on-axis loading, $\alpha_{max} = 11\cdot58$ for $\vartheta = 0°$; (d) off-axis loading, $\alpha_{max} = 3\cdot21$ for $\vartheta = 6\cdot9°$; $\alpha_{min} = -2\cdot73$ for $\vartheta = 172\cdot8°$. Material constants C-fibre reinforced borosilicate glass:[15] $E_{||} = 169\,\mathrm{GPa}$; $E_{\perp} = 32\,\mathrm{GPa}$; $v_{||\perp} = 0\cdot18$; $G_{*} = 22\,\mathrm{GPa}$.
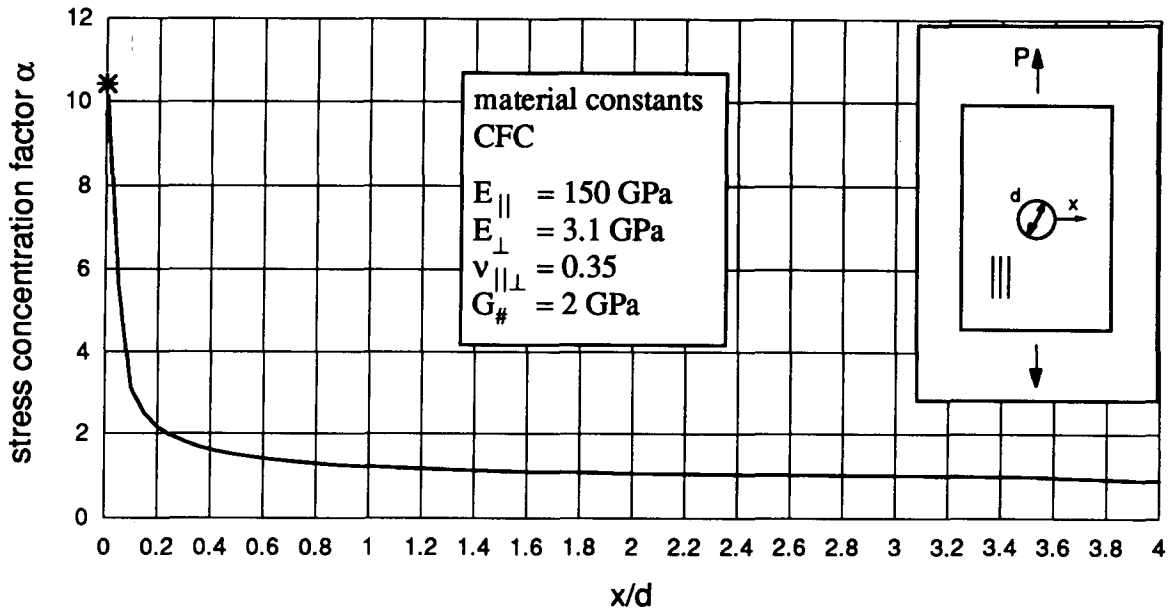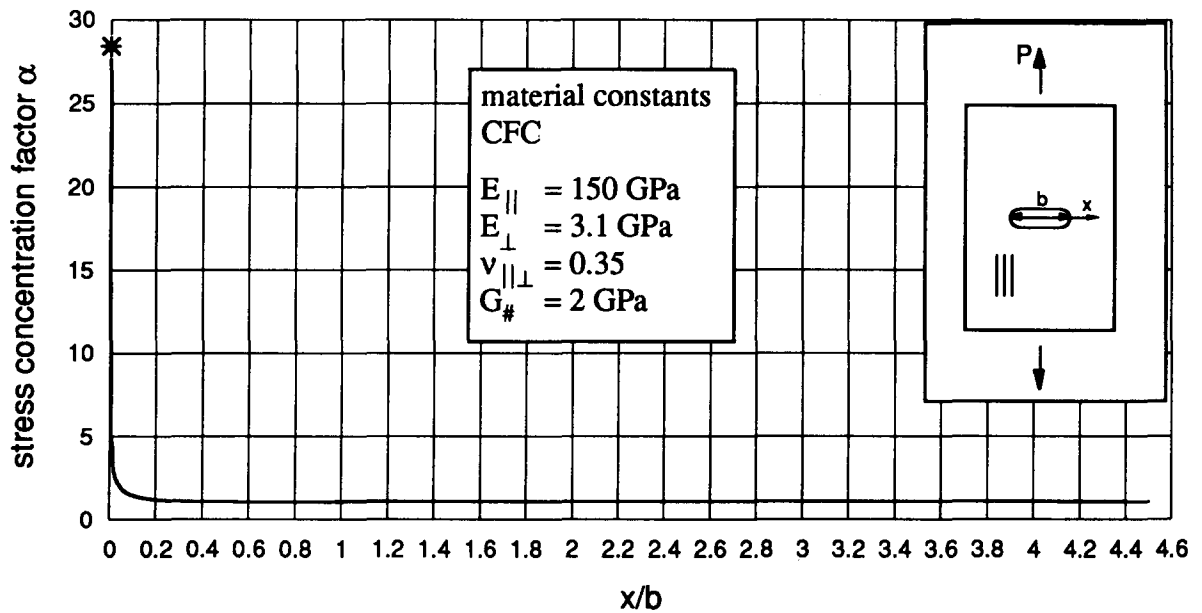
Fig. 7. Decrease of stress concentration maxima for (a) a circular notch and (b) an oblong hole (FEM-calculations).

7 Conclusion and Proposals for Future Work

In high-tech ceramic components used in engineering, holes are often required for reasons of design. Because of local stress concentrations under tension, these holes are the actual weak points of ceramic structures. Even small loads can cause catastrophic failure in the vicinity of these notches.

For these reasons, holes susceptible to failure require an individual treatment on the basis of mechanical analysis. First of all, this statement is applicable to anisotropically fibre-reinforced ceramics in cases where the direction of the applied

tension and the direction of the fibres do not coincide (off-axis loading). In these cases the origin of failure is usually not situated at the notch root. Furthermore, an increase in the degree of anisotropy $(E_{\parallel}/E_{\perp})$ is accompanied by an increase of the stress concentration factor.

Further thorough investigations of the failure mode of a fibre–matrix composite, besides the stress concentration analysis, are necessary for correct dimensioning of components. During this development a special emphasis must be placed on the establishment of suitable failure criteria, since the orientational dependence of both strength and

toughness of the material has to be considered in this case.

The preceding explanations have pointed out the necessity of establishing a mathematical basis to assist the development of fibre-reinforced ceramics and their successful technical application.

References

1. Menges, G. & Ziegler, G., Faserverbundwerkstoffe, Grundlagen und Einführung in die Besonderheiten. In *BMFT-Symposium Materialforschung 1988*, Hamm, 12–14 September 1988, Projektleitung Material- und Rohstofforschung, KFA Jülich GmbH, pp. 57–128.
2. Kromp, K., Bruchmechanik und Festigkeitsverhalten von keramischen Verbundwerkstoffen. In *Proceedings Verbundwerk 88*, Wiesbaden, 19–22 September 1988, ed. S. Schnabel, R. Gadow & J. Kriegesmann. Distributed by Demat Exposition Managing, Frankfurt/Main, pp. 36.00–36.26.
3. Krenkel, W., Möglichkeiten und Grenzen faserverstärkter Keramiken. In *Seminar Deutsche Keramische Gesellschaft*, Stuttgart, 19–20 March 1991, DKG-Seminar 'Materialgerechtes Design für keramische Bauteile'.
4. Gerhardy, Th., Institute of Technical Mechanics, Technical University of Clausthal, personal communications, 1991.
5. Bunsell, A. R., Fibres for metallic and ceramic composites, the scientific aspects and their relation to composite performances. In *RISO Symposium 9*, ed. S. I. Andersen, H. Lilholt & O. B. Pedersen, Risø National Laboratory, Roskilde, Denmark, 1988, pp. 1–12.
6. Fitzter, E. & Remmele, W., Faserverbundwerkstoffe zur Anwendung bei hohen Temperaturen. *Technische Keramik Handbuch*, 2nd Issue. Vulkan Verlag, Essen, 1990, pp. 91–103.
7. Prewo, K. M., Tension and flexural strength of silicon carbide fibre-reinforced glass ceramics. *J. Mater. Sci.*, **21** (1986) pp. 3590–600.
8. Hufenbach, W. & Kroll, L., Kerbspannungsprobleme anisotrop faserverstärkter Scheiben. In *Annual Scientific Meeting of the Gesellschaft für Angewandte Mathematik und Mechanik*, Krakow, 2–5 April 1991.
9. Hufenbach, W., Schäfer, M. & Herrmann, A. S., Berechnung des Spannungs- und Verschiebungsfeldes anisotroper Scheiben mit elliptischem Ausschnitt. *Ingenieur-Archiv*, **60** (1990) pp. 507–17.
10. Hufenbach, W. & Kroll, L., Kerbspannungsprobleme anisotrop faserverstärkter Scheiben. *Ingenieur-Archiv*, **62** (1992) pp. 277–90.
11. Hufenbach, W., Schäfer, M. & Herrmann, A. S., Photoelastische Dehnungsmessung und Spannungsermittlung an faserverstärkten Bauteilen. *Kunststoffe*, **81**(1) (1991) pp. 76–80.
12. Kroll, L., Institute of Technical Mechanics, Technical University of Clausthal, Internal Report, 1991.
13. Hufenbach, W. & Kroll, L., Der verschiedenartige Einfluß unterschiedlicher Kerbformen bei Faserverbundwerkstoffen. In *WG Composite Research in Solid Mechanics*, Stuttgart, 5–6 December 1991.
14. Herrmann, A. S., Experimentelle und theoretische Untersuchungen von Kerbspannungsproblemen anisotrop glasfaserverstärkter Epoxidharzscheiben. Dissertation, Institute of Technical Mechanics, Technical University of Clausthal, 1989.
15. Nardone, V. C. & Prewo, K. M., Tensile performance of carbon-fibre-reinforced glass. *J. Mater. Sci.*, **23** (1988) pp. 168–80.
16. Kolshorn, K.-U., Institute of Technical Mechanics, Technical University of Clausthal, personal communications, 1991.